# Fabrication of ZnO/Graphene Nanocomposite by Ultrasonic Homogenization

Jacob D. Pfund[1]
*Department of Physics*
*University of Wisconsin - La Crosse*
*La Crosse, WI*

## Abstract

Indium tin oxide (ITO) is a commonly used material in the production of transparent conducting films. However, indium is toxic, environmentally unfriendly, and expensive. To remedy this issue, a new material must be developed which can serve as a replacement for ITO. This project utilized commercially available zinc oxide powder and graphene nanoplatelets to manufacture nanocomposite materials through ultrasonic homogenization. To investigate their physical properties, these nanocomposites were then subjected to UV-Vis spectroscopy, particle size analysis, scanning electron microscopy, and X-ray diffractometry. Results indicate that ZnO/Graphene nanocomposites have promising potential as an inexpensive and environmentally friendly transparent conductor.

## Introduction

From harvesting solar energy to personal electronics to biomedical sensors, transparent conducting materials play a critical role in today's technology. Currently, the most commonly used transparent conductor is indium-tin oxide (ITO) (Du et al. 2014). However, the widespread use of ITO poses several issues. For one, indium is toxic to blood, kidneys, reproductive system, liver, heart, upper respiratory tract, skin, and eyes (Cummings et al. 2012). Additionally, indium is a possible environmental hazard if not disposed of properly. Moreover, ITO is as rare as silver in the Earth's crust (Frenzel et al. 2017). For these reasons it is crucial that a less expensive, more environmentally friendly alternative be developed, ideally utilizing conventional manufacturing tools and processing techniques.

One possible alternative material is a combination of zinc oxide (ZnO) and graphene. ZnO is a well-studied compound that finds use in a wide variety of applications, from rubber production to baby powder, and is even found in everyday breakfast cereal (Volz 2006). While it is inexpensive, environmentally friendly, and able to easily coat large surfaces, ZnO has poor electrical conductivity on its own. This makes it difficult to use as a transparent conducting material and often results in ZnO being alloyed with another material, such as indium, to decrease its resistance (Özgür et al. 2005).

Graphene is a sheet of carbon atoms only one layer thick and arranged in a hexagonal lattice structure. Graphene has recently gathered a large amount of attention due to its unique properties such as high electrical conductivity, optical transparency, enormous breaking strength, and non-toxicity on the nanoscale (Geim 2009; Talukdar et al. 2014). However, graphene's two dimensional structure renders it brittle and difficult to manufacture as a single large sheet more than a few nanometers across. So while graphene is an excellent transparent conductor on its own, it is nearly impossible to manufacture large sheets on an industrial scale.

By combining ZnO and graphene into a nanocomposite material via ultrasonic homogenization, it should be possible to manufacture a material which exhibits the beneficial properties of both constituents. In particular, adjusting the homogenization time it should result in nanocomposite

[1]Funding for this project was provided by the Wisconsin Space Grant Consortium. Lab equipment, mentoring, and materials were supplied by Dr. Seth King and the University of Wisconsin-La Crosse. A special thanks goes out to Dr. King and Avery McLain for their invaluable guidance and support throughout this project.

materials which retain the high optical transparency and electrical conductivity of graphene, while also being easy to deposit as a thin film. Finally, by utilizing ultrasonic homogenization there should be no unwanted chemical reactions between ZnO and graphene which would result in the presence of a completely new compound and therefore change the properties of the nanocomposite.

**Methods**

ZnO powder and graphene nanoplatelets were purchased from Alpha Aesar and used as delivered. Two separate sets of dispersions, one of 0.05 M ZnO and another containing 0.2 g/L graphene, were prepared using Millipore $H_2O$. A third set of dispersions containing both 0.05 M ZnO and 0.2 g/L graphene (ZnO/G) was also prepared. Dispersions were then subdivided into 20 mL glass vials for easy handling. All three sets of dispersions were subjected to ultrasonic homogenization for a selection of times ranging from 0 to 30 minutes. Sonication was performed in 10 minute increments using a Fisher 550 Sonic Dismembrator at 15% power to prevent heating the dispersions to boiling. After homogenization, dispersions were allowed to settle in their vials at room temperature for 24 hours before analysis.

A Cary 5000 UV-Vis-NIR spectrophotometer was used to study the optical absorption profiles of all three types of solutions. Dispersions were loaded into fused quartz fluorescence cuvettes and their optical absorbance was recorded at room temperature for wavelengths ranging from 200 nm to 800 nm. Particle size measurements were then performed using a Malvern Zetasizer Nano-ZS and the same quartz cuvettes at room temperature. Cuvettes were cleaned between uses by nitric acid bath for a minimum of 3 hours to remove any residual particles still present inside. After the bath, cuvettes were rinsed with Millipore $H_2O$ to remove the remaining acid.

Two homogenized ZnO/G dispersions, sonicated for 15 and 30 minutes respectively, were centrifuged at 4000 rpm for 20 minutes and the supernatant poured off. In both cases, the remaining pellet of sonicated ZnO/G was then redispersed in acetone. A single-crystal silicon wafer was heated to 90°C and the new acetone dispersion drop cast onto it to form a thin film of ZnO/G. A Siemens D500 diffractometer was used to perform X-ray Diffraction (XRD) on the thin films in order to analyze the integrity of the homogenized ZnO crystals and graphene nanoplatelets. In addition, scanning electron microscopy (SEM) was performed using a Zeiss EVO HD unit to obtain images of the ZnO/G thin films.

**Results**

Fig. 1 shows the absorbance spectra of several prepared ZnO dispersions for a range of sonication times. Two significant features were observed: the broad peak from 235 nm to 283 nm which peaks at 254 nm, as well as the trough at 210 nm. The unhomogenized dispersion (0 min) does not exhibit the broad peak present in the other samples, but does retain a slight feature around 210 nm and shares the observed drop in absorbance at 235 nm. Finally, the slight jump seen at 350 nm is due to a bulb change within the spectrophotometer.

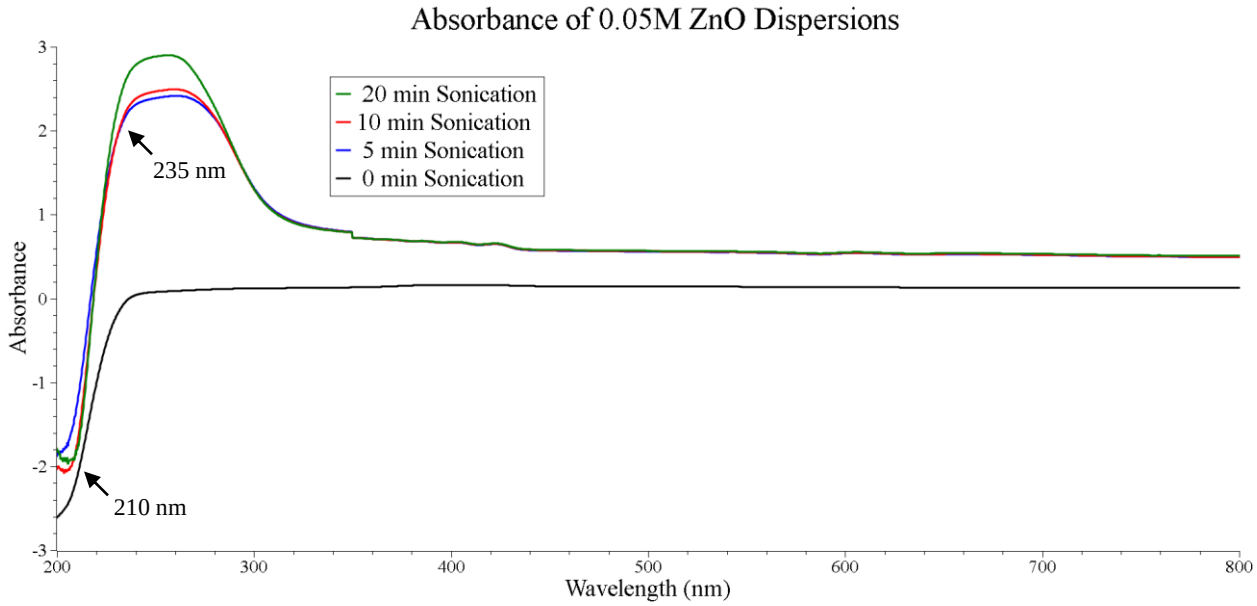


Fig. 1: Absorbance spectra of ZnO dispersions at varying degrees of homogenization. Arrows indicate the locations of both significant features.

The absorbance spectra of graphene dispersions sonicated identically to the dispersions featured in Fig. 1 are displayed below in Fig. 2. Here, the major feature has a more gradual onset and its location varies slightly. As sonication time increases, the peak blue shifts by approximately 5 nm, from 273 nm to 268 nm. Such a blue shift indicates a reduction in the average particle size of the dispersion (Pesika et al. 2003).

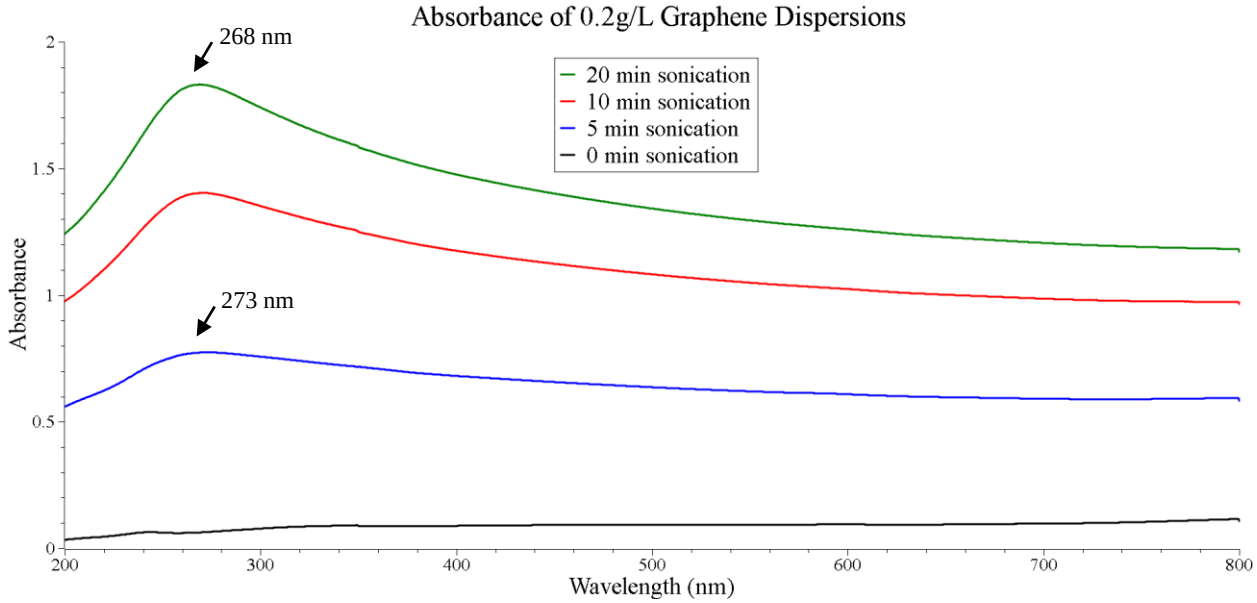


Fig. 2: Absorbance spectra of graphene dispersions at varied degrees of homogenization. A 5 nm blue shift in the peak location occurs as sonication time increases.

Fig. 3 displays the observed absorbance spectra of the homogenized ZnO/G dispersions. The spectra retain several features similar to the ZnO dispersions, such as the 283 nm hump and 235 nm trough. The feature at approximately 205 nm is also likely due to ZnO, however the reason for its 5 nm shift and inversion from Fig. 1 is unknown. The peaks present around 252 nm experience a 5 nm blue shift from 0 to 20 minutes of sonication time, which mirrors the shift observed in Fig. 2. This blue shift indicates that the 252 nm peaks are caused by the presence of graphene rather than ZnO.

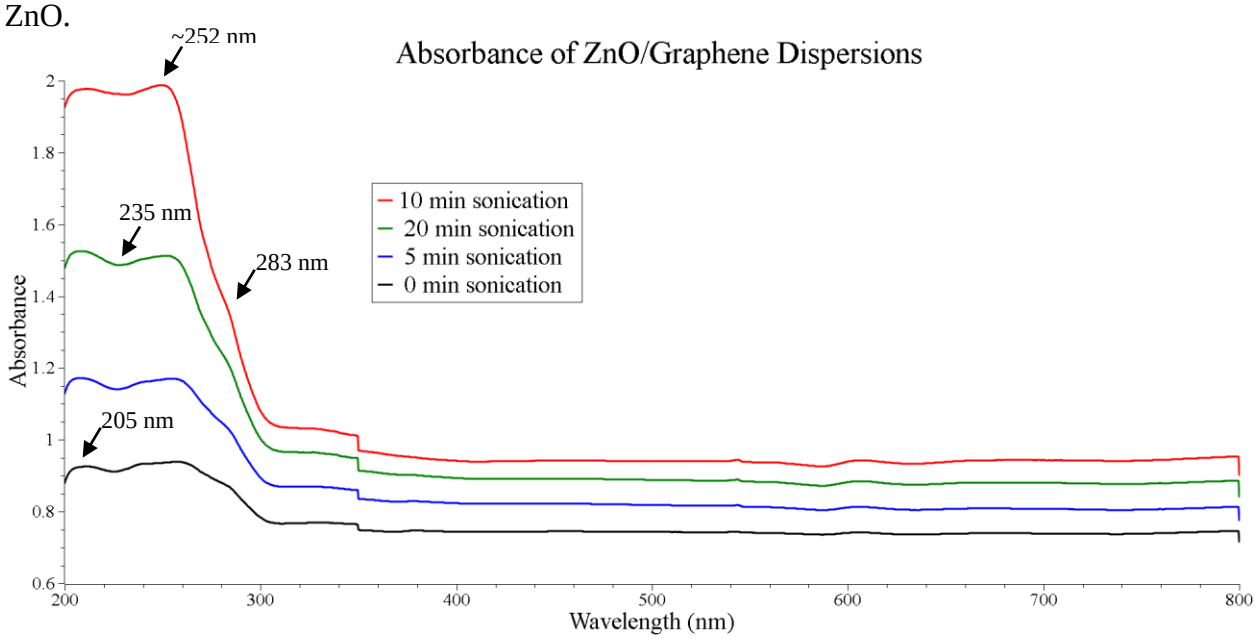


Fig. 3: Absorbance spectra of ZnO/G dispersions at varied degrees of homogenization. The locations of several notable features are marked with arrows.

The average particle size of all three dispersion sets with relation to homogenization time is shown below in Fig. 4. From this data it is apparent that sonication time does indeed reduce the average particle size of the graphene and ZnO/G dispersions, as previously indicated by the blue shift observed in Figs. 2 and 3. Additionally, while particles in the graphene and ZnO/G sets experienced a fairly constant reduction in size, pure ZnO particles varied greatly between each dispersion. The precise reason for this in unknown, but it is suspected that the dispersed ZnO powder experienced more significant agglomeration during the 24 hour settling period before analysis, resulting in greater variation between samples.

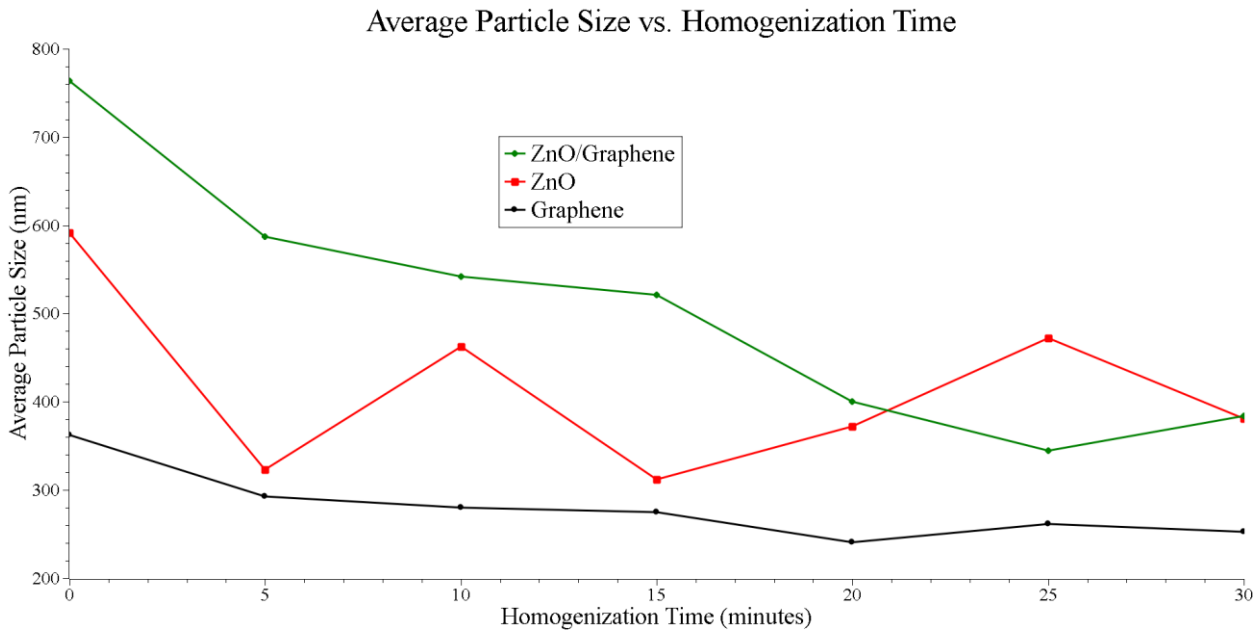

Fig. 4: Average particle size recorded for all three dispersion sets after sonicating for a variety of times.

Thin films were fabricated by drop casting two ZnO/G dispersions which had been sonicated for 15 and 30 minutes respectively. A total of four SEM images were taken of these films, with an EHT value of 15 kV, and are shown in Fig. 5. Several holes can be seen in 5(a) which suggests that the film is of poor quality. In contrast, the 30 minute film shown in 5(c) is considerably more uniform with only a single notable gap near the lower right corner. However it is also of note that 5(a) contains a large deformity in the upper right corner, this is likely due to a stray dust particle and is not representative of the entire film.

(a) 15 min at 750x mag.

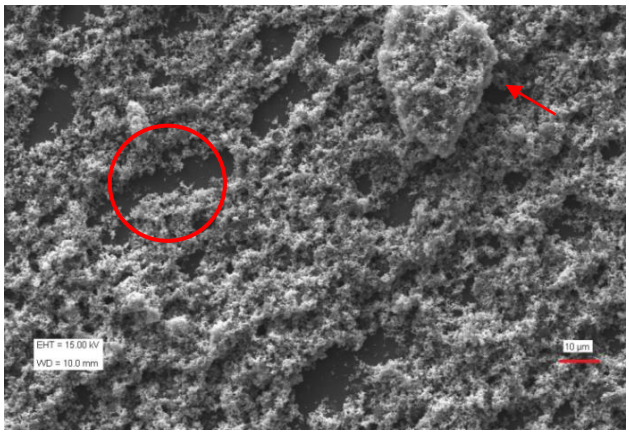


(b) 15 min at 3000x mag.

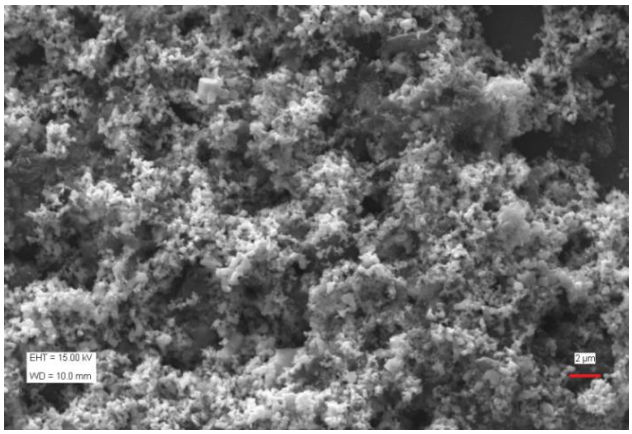


(c) 30 min at 750x mag.

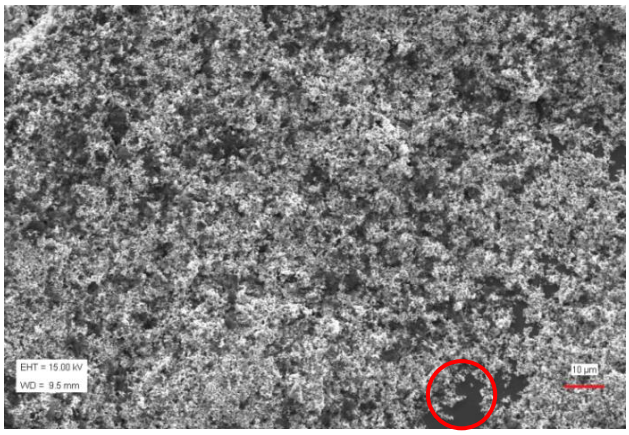


(d) 30 min at 3000x mag.

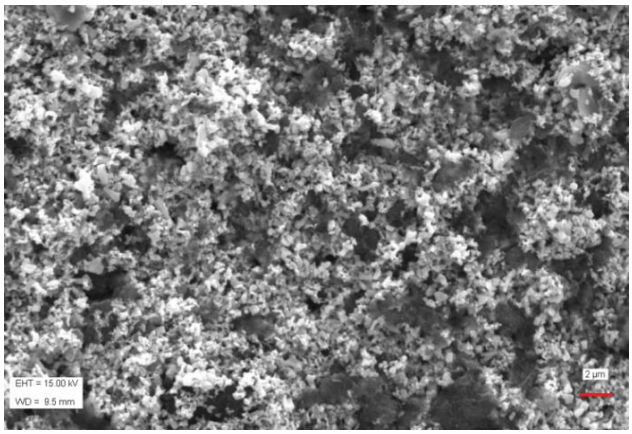


Fig. 5: SEM images of drop cast ZnO/G nanocomposite thin films after homogenization. Each film is shown at both 750x and 3000x magnification. Gaps in the films show up as dark grey areas (examples are circled in red). The arrow indicates a stray dust particle.

X-ray Diffraction was performed to analyze the crystalline structures present in the films; the results are displayed in Fig. 6 below. The major peaks seen from 30 to 70 degrees are in agreement with the JCPDS file on ZnO. It is also clear that the nanocomposite contained hexagonal wurtzite ZnO with no significant crystalline impurities (Selvarajan and Mohanasrinivasan 2013; Saleh et al. 2017). These two observations reveal that the crystalline structure of ZnO is undamaged by both ultrasonication and the drop casting process. Finally, the minor feature located at 26 degrees is due to the presence of graphite, with the 30 minute film's peak being slightly wider and less intense than the 15. This indicates that domain size is decreasing with sonication time, as previously shown by both the UV-Vis and particle size data shown above.

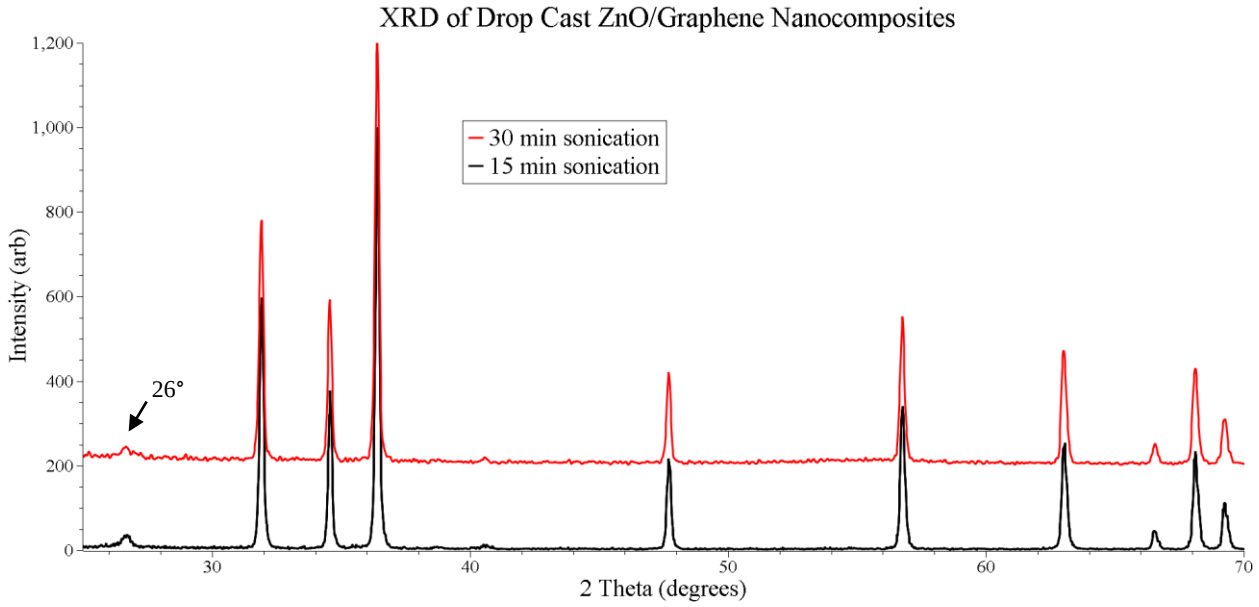


Fig. 6: XRD patterns of drop cast ZnO/G dispersions (vertical offset of 200).

## Conclusions

The experimental results reported above indicate that ultrasonic sonication is a potential large-scale manufacturing technique for ZnO/G nanocomposites. From the UV-Vis data in Figs. 1 – 3 it can be concluded that no new chemical compounds are formed during the sonication process. In addition, the particle sizing results shown in Fig. 4 demonstrate that sonicating ZnO/G dispersions in $H_2O$ significantly reduces the size of nanoparticles present. These two findings indicate that graphene exfoliation may be occurring during the sonication process, as the energy required to separate layers of graphene from one another is significantly less than what is required to break bonds within the layers (Wang et al. 2015). This suggests that the proposed method of fabrication is not only inexpensive, but feasible with multi-layer graphene rather than more expensive single-layer graphene.

XRD data from the ZnO/G films, seen in Fig. 6, shows that the crystalline structure of ZnO is not compromised during sonication. This allows ZnO to retain its beneficial properties, such as its ability to easily coat large surfaces. The SEM images of prepared ZnO/G films presented in Fig. 5(a) and 5(c) clearly show a drastic increase in film uniformity with sonication time. As structural consistency plays a key role in a thin conducting film's ability to function, this improvement is a major benefit resulting from the proposed manufacturing technique (Kim et al. 2000).

As of now, it is difficult to determine the exact nature of the crystalline structures present in the films without more information. This study could be further expanded by examining the fluorescence profiles of ZnO, graphene, and ZnO/G dispersions to clarify the interaction between ZnO crystals and graphene particles. Analysis of the optical transmittance, electrical resistivity and breaking strength of ZnO/G thin films is also an important next step towards determining their viability as a transparent conducting material. If these ZnO/G thin films exhibit high optical transmittance and electrical conductivity, they would be a cost-effective alternative to ITO with the added benefits of being non-toxic and environmentally friendly.

## References


Cummings, K. J., Nakano, M., Omae, K., Takeuchi, K., Chonan, T., Xiao, Y., . . . Kreiss, K. (2012). Indium Lung Disease. Chest,141(6), 1512-1521. doi:10.1378/chest.11-1880

Debanath, M., & Karmakar, S. (2013). Study of blueshift of optical band gap in zinc oxide (ZnO) nanoparticles prepared by low-temperature wet chemical method. Materials Letters, 111, 116-119. doi:10.1016/j.matlet.2013.08.069

Du, J., Chen, X., Liu, C., Ni, J., Hou, G., Zhao, Y., & Zhang, X. (2014). Highly transparent and conductive indium tin oxide thin films for solar cells grown by reactive thermal evaporation at low temperature. Applied Physics A, 117(2), 815-822. doi:10.1007/s00339-014-8436-x

Frenzel, M., Mikolajczak, C., Reuter, M. A., & Gutzmer, J. (2017). Quantifying the relative availability of high-tech by-product metals – The cases of gallium, germanium and indium. Resources Policy, 52, 327-335. doi:10.1016/j.resourpol.2017.04.008

Geim, A. K. (2009). Graphene: Status and Prospects. Science, 324(5934), 1530-1534. doi:10.1126/science.1158877

Kim, H., Horwitz, J. S., Kushto, G., Piqué, A., Kafafi, Z. H., Gilmore, C. M., & Chrisey, D. B. (2000). Effect of film thickness on the properties of indium tin oxide thin films. *Journal of Applied Physics, 88*(10), 6021-6025. doi:10.1063/1.1318368

Özgür, Ü., Alivov, Y. I., Liu, C., Teke, A., Reshchikov, M. A., Doğan, S., . . . Morkoç, H. (2005). A comprehensive review of ZnO materials and devices. Journal of Applied Physics, 98(4), 041301. doi:10.1063/1.1992666

Pesika, N. S., Stebe, K. J., & Searson, P. C. (2003). Relationship between Absorbance Spectra and Particle Size Distributions for Quantum-Sized Nanocrystals. The Journal of Physical Chemistry B, 107(38), 10412-10415. doi:10.1021/jp0303218

Saleh, S. M., Soliman, A. M., Sharaf, M. A., Kale, V., & Gadgil, B. (2017). Influence of solvent in the synthesis of nano-structured ZnO by hydrothermal method and their application in solar-still. Journal of Environmental Chemical Engineering, 5(1), 1219-1226. doi:10.1016/j.jece.2017.02.004

Selvarajan, E., & Mohanasrinivasan, V. (2013). Biosynthesis and characterization of ZnO nanoparticles using Lactobacillus plantarum VITES07. Materials Letters, 112, 180-182. doi:10.1016/j.matlet.2013.09.020

Talukdar, Y., Rashkow, J. T., Lalwani, G., Kanakia, S., & Sitharaman, B. (2014). The effects of graphene nanostructures on mesenchymal stem cells. Biomaterials, 35(18), 4863-4877. doi:10.1016/j.biomaterials.2014.02.054

Völz, H. G. (2006). Ullmann's Encyclopedia of Industrial Chemistry. doi:10.1002/14356007.a20_243.pub2

Wang, W., Dai, S., Li, X., Yang, J., Srolovitz, D. J., & Zheng, Q. (2015). Measurement of the cleavage energy of graphite. Nature Communications, 6, 7853. doi:10.1038/ncomms8853